ELSEVIER

Journal of Crystal Growth 242 (2002) 491–500

JOURNAL OF CRYSTAL GROWTH

www.elsevier.com/locate/jcrysgro

Instabilities in liquid metals controlled by constant magnetic field—Part I: vertical magnetic field

S. Kaddeche[a], D. Henry[b,*], T. Putelat[b], H. Ben Hadid[b]

[a] *Institut National des Sciences Appliquées et de Technologie, B.P. 676 – 1080 Tunis Cedex, Tunisia*

[b] *Laboratoire de Mécanique des Fluides et d'Acoustique, UMR-CNRS 5509, Ecole Centrale de Lyon, Université Claude Bernard, Lyon 1, B.P. 163–69131 Ecully Cedex, France*

Received 24 December 2001; accepted 1 May 2002

Communicated by D.T.J. Hurle

Abstract

We investigate the stabilizing effects of a constant vertical magnetic field on the flow in a heated planar liquid metal layer. The steady shear flow driven in the bounded layer by the imposed horizontal temperature gradient can involve two types of instability: stationary transverse instabilities and oscillatory longitudinal instabilities. The performed approximate analytical linear stability analysis shows that the vertical magnetic field has a great stabilizing effect on both types of instability with variations of the thresholds (critical Grashof numbers) as $Gr_c - Gr_c(Ha = 0) \propto Ha^2$ for the longitudinal instabilities and as $Gr_c \propto \exp(Ha^2/21.6)$ for the transverse instabilities (Ha is the Hartmann number proportional to the intensity of the magnetic field). Both instabilities also disappear beyond a limit value of Ha. These results could be of great interest for crystal growers as the vertical field is seen to delay the onset of instabilities, in particular the oscillatory instabilities which are responsible for the appearance of undesirable striations in the grown crystals.

PACS: 47.20; 47.32; 47.65

Keywords: A1. Instability; A1. Magnetic fields; A1. Thermally induced flow

1. Introduction

Convection in a horizontal metallic liquid layer subject to a horizontal temperature gradient received considerable attention due to its relevance to several material processing technologies, like semiconductor crystal growth from a melt. It is well known that the transition from stationary flow to time dependent flow occurs when the horizontal temperature gradient (Rayleigh number) exceeds a certain critical threshold, and that this transition greatly affects the grown crystal properties. In material processing facilities, static magnetic field is used for contactless control of fluid flow and thus of heat and mass transport during the process. It was shown experimentally [1–3] that static magnetic field can lead to the suppression of the temperature fluctuations. Thus,

*Corresponding author. Tel.: +33(0)4-72-18-61-70; fax: +33(0)4-78-64-71-45.

E-mail address: henry@mecaflu.ec-lyon.fr (D. Henry).

0022-0248/02/$ - see front matter
PII: S0022-0248(02)01427-6

the use of magnetic field appears to be a promising way to damp the oscillations and stabilize the flow, and thus to improve the quality of the grown crystal.

A significant literature based on the linear stability analysis treated the problem of the development of instabilities in a liquid layer subject to a horizontal temperature gradient, either analytically [4] or numerically [5–12]. Some of these studies included the effect of a vertical magnetic field, the first papers on the subject being due to Russian teams [5,6]. Ben Hadid et al. [11] have shown the stabilization induced by a constant vertical magnetic field on buoyancy driven flows in open cavities with a stress free upper surface. Priede and Gerbeth [12] have investigated the situation where the flow is driven by surface tension. They have shown that the vertical magnetic field is very effective in stabilizing the hydrothermal waves which appear in this situation, and have established several scaling laws.

In the present paper we study the effect of a constant vertical magnetic field on both stationary transverse and oscillatory longitudinal instabilities. These two types of instabilities were already observed in the case without magnetic field [4,7,8,10,11]. For the oscillatory longitudinal instabilities, we follow the approximate analytical approach developed by Gill [4], whereas for the stationary transverse instabilities, the approach is based on a Taylor development. The case of a horizontal magnetic field is considered in the companion paper [13].

2. Governing equations and laminar basic flow

We consider the flow of viscous, electrically conducting, incompressible fluid induced by a horizontal temperature gradient in an infinite horizontal layer which is subject to an external uniform vertical magnetic field $\vec{B}_0 = B_0\vec{e}_z$ (see Fig. 1). All the properties of the fluid are assumed to be constant, except for the density in the buoyancy term which obeys the classical Boussinesq law: $\rho = \rho_0\,[1 - \beta(T - T_0)]$ where β is the thermal expansion coefficient.

The magnetic field acting on the fluid flow is $\vec{B} = \vec{B}_0 + \vec{b}$, where $\vec{b}$ is the induced magnetic field. Since the magnetic Reynolds number, Re_m, of most liquid metals used in crystal growth applications are very small ($Re_m \approx 10^{-3}$), we can neglect the induced magnetic field and consider that $\vec{B} = \vec{B}_0$. The layer of depth H is bounded from below and above by horizontal plane boundaries.

The conservation equations of momentum, mass, heat and charge are made dimensionless using H, H^2/ν, ν/H, $H\nabla T$ and $\nu\|\vec{B}_0\|$ as scale quantities for length, time, velocity, temperature and induced electric potential, respectively (∇T is the temperature gradient imposed by the heating facility). The dimensionless governing equations can be written as follows:

$$\frac{\partial \vec{V}}{\partial t} + (\vec{V}\cdot\vec{\nabla})\vec{V} = -\vec{\nabla}P + \nabla^2\vec{V} + Gr\,T\vec{e}_z + Ha^2(-\vec{\nabla}\Phi + \vec{V}\times\vec{e}_{B_0})\times\vec{e}_{B_0}, \tag{1}$$

$$\vec{\nabla}\cdot\vec{V} = 0, \tag{2}$$

$$\frac{\partial T}{\partial t} + \vec{V}\cdot\vec{\nabla}T = \frac{1}{Pr}\nabla^2 T, \tag{3}$$

$$\nabla^2\Phi = (\vec{\nabla}\times\vec{V})\cdot\vec{e}_{B_0}, \tag{4}$$

where $\vec{e}_{B0} = \vec{B}_0/\|\vec{B}_0\|$ is the unit vector indicating the direction of $\vec{B}_0$ and Φ is the dimensionless electric potential. The dimensionless parameters appearing in Eqs. (1) and (3) are: $Gr = g\beta\nabla T H^4/\nu^2$, the Grashof number, $Ha = \|\vec{B}_0\|\,H\sqrt{\sigma_e/\rho_0\nu}$, the Hartmann number ($\sigma_e$ is the electric conductivity of the liquid metal), and $Pr = \nu/\kappa$, the Prandtl number. In the momentum conservation equation, the body force $Ha^2\left(-\vec{\nabla}\Phi + \vec{V}\times\vec{e}_{B_0}\right)\times\vec{e}_{B_0}$ represents the Lorentz force, consequence of the interaction of the induced electric current density and the external applied magnetic field $\vec{B}_0$. Let us note that Eq. (4) is obtained from the conservation of the induced electric current given by Ohm's law.

If the liquid layer is assumed to be infinitely long, the set of Eqs. (1)–(4) admits a stationary parallel flow solution $\vec{V} = (U_0(z), 0, 0)$. This solution is governed by the following reduced

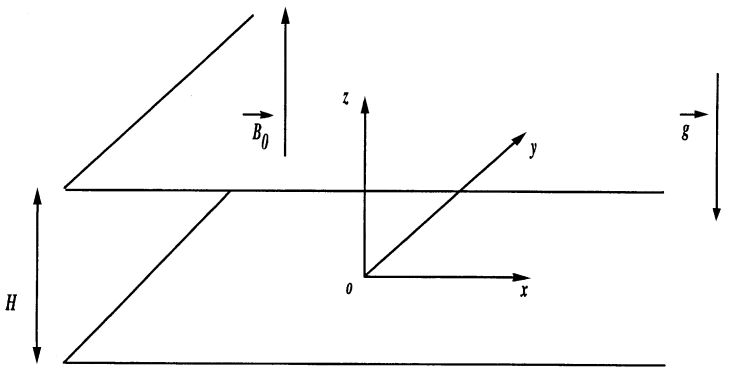

Fig. 1. Studied configuration.

system:

$$\frac{d^3U_0}{dz^3} - Ha^2\frac{dU_0}{dz} - Gr = 0, \tag{5}$$

$$\frac{d^2T_0}{dz^2} = Pr\,U_0. \tag{6}$$

For a vertical coordinate z, $-\frac{1}{2}\leqslant z\leqslant\frac{1}{2}$, the solution of Eq. (5) is:

$$U_0(z) = \frac{Gr}{Ha^2}\left(\frac{\sinh(Ha\,z)}{2\sinh(Ha/2)} - z\right). \tag{7}$$

The temperature profile, solution of Eq. (6), writes for thermally conducting boundaries,

$$T_0(x,z) = x + \frac{Gr\,Pr}{Ha^2}\left(\frac{\sinh(Ha\,z)}{2Ha^2\sinh(Ha/2)} - \frac{z^3}{6} + \left(\frac{1}{24} - \frac{1}{Ha^2}\right)z\right), \tag{8}$$

and for thermally insulating boundaries,

$$T_0(x,z) = x + \frac{Gr\,Pr}{Ha^2}\left(\frac{\sinh(Ha\,z)}{2Ha^2\sinh(Ha/2)} - \frac{z^3}{6} + \left(\frac{1}{8} - \frac{\cosh(Ha/2)}{2Ha\sinh(Ha/2)}\right)z\right). \tag{9}$$

3. Linear stability analysis for the oscillatory longitudinal instabilities

The shear flow described by Eqs. (7)–(9) is known to be unstable at sufficiently large values of the Grashof number. In this section, we focus on the oscillatory longitudinal instabilities defined by a zero wavenumber along x and corresponding to a three-dimensional mode which consists of rolls with the axis parallel to the basic flow. It has to be noted that without magnetic field the longitudinal mode is not the most unstable for the lower values of Pr. We analyze the linear stability of the basic state (7)–(9) with respect to infinitesimal disturbances in the form of plane travelling waves along y. Let the velocity perturbation be (u, v, w), the temperature perturbation be θ, and the induced electric potential perturbation be ϕ. We can write the components of the velocity perturbation in the (yOz)-plane as a function of a stream function ψ:

$$v = -\psi_z \quad \text{and} \quad w = \psi_y. \tag{10}$$

The governing equations for the perturbation become:

$$\theta_t + uT_{0x} + \psi_y T_{0z} = \frac{1}{Pr}\Delta\theta, \tag{11}$$

$$u_t + \psi_y U_{0z} = \Delta u - Ha^2(u + \phi_y), \tag{12}$$

$$\Delta\psi_t = Gr\,\theta_y + \Delta^2\psi - Ha^2\psi_{zz}, \tag{13}$$

where $\Delta = \partial^2/\partial y^2 + \partial^2/\partial z^2$ and Eqs. (11)–(13) are respectively the energy equation, the x component of the momentum equation and the x component of the vorticity equation. The induced electric potential perturbation ϕ which acts in Eq. (12), can be obtained through the induced electric current continuity equation deduced from Eq. (4) which can be written here as

$$\Delta\phi = -u_y. \tag{14}$$

Eq. (13) gives θ_y in terms of ψ. The substitution of the obtained equation into the y derivative of Eq. (11) results in an equation for the derivative of the longitudinal velocity component, u_y:

$$-Gr\,u_y T_{0x} = \left(\frac{\partial}{\partial t} - \Delta\right)\left(\frac{\partial}{\partial t} - \frac{1}{Pr}\Delta\right)\Delta\psi + Ha^2\left(\frac{\partial}{\partial t} - \frac{1}{Pr}\Delta\right)\psi_{zz} + Gr\,T_{0z}\psi_{yy}. \quad (15)$$

Taking the y derivative of Eq. (12) and applying the laplacian operator in order to eliminate ϕ by using Eq. (14), u_y can be obtained as a function of ψ:

$$A\ u_y = -\Delta\ \psi_{yy}\ U_{0z}, \quad (16)$$

with

$$A = \left(\frac{\partial}{\partial t} - \Delta + Ha^2\right)\Delta - Ha^2\frac{\partial^2}{\partial y^2}. \quad (17)$$

The substitution of u_y obtained from Eq. (15) into Eq. (16) leads to an equation in terms of ψ:

$$\left(\frac{\partial}{\partial t} - \Delta\right)\left(\frac{\partial}{\partial t} - \frac{1}{Pr}\Delta\right)\ A\ \Delta\psi + Gr\,A\ T_{0z}\ \psi_{yy} - Gr\ T_{0x}\ \Delta\ U_{0z}\ \psi_{yy} + Ha^2\ \left(\frac{\partial}{\partial t} - \frac{1}{Pr}\Delta\right)\ A\ \psi_{zz} = 0. \quad (18)$$

In the particular case of longitudinal instability, the general solution of Eq. (18) may be written as

$$\psi = e^{\sigma t}\sin(\ell y)\eta(z), \quad (19)$$

where ℓ is the wavenumber in the y direction and σ is a complex growth rate. Substituting (19) into (18) leads to an ordinary differential equation of order ten in z, namely

$$(\sigma - \Delta)\ \left(\sigma - \frac{1}{Pr}\Delta\right)\ A_1\ \Delta\eta - \ell^2\,Gr\,A_1\ T_{0z}\ \eta + \ell^2\ Gr\ T_{0x}\ \Delta\ U_{0z}\ \eta + Ha^2\ \left(\sigma - \frac{1}{Pr}\Delta\right)\ A_1\ \eta_{zz} = 0, \quad (20)$$

where $\Delta = -\ell^2 + d^2/dz^2$, and $A_1 = (\sigma - \Delta + Ha^2)\ \Delta + Ha^2\ \ell^2$. As it can be seen from Eqs. (7)–(9), U_{0z} is proportional to Gr while T_{0z} is proportional to $Gr\,Pr$, and $T_{0x} = 1$. Consequently, we can write that $U_{0z} = Gr\,v_z(z)$ and $T_{0z} = Gr\,Pr\,\tau_z(z)$. As done by Gill [4] approximate solutions of (20) can be obtained by replacing $v_z(z)$ and $\tau_z(z)$ by adequate constants $\bar{v}_z$ and $\bar{\tau}_z$ which can be chosen as appropriately weighted mean values of $v_z(z)$ and $\tau_z(z)$. The values of the constants $\bar{v}_z$ and $\bar{\tau}_z$ obtained with $\cos^2(\pi z)$ as weighting function are given in Appendix A for different boundary conditions. The precision of this approximation will depend on the suitability of the used weighting function. At worst, this method can be considered as a form of scaling analysis giving the dependence of the threshold parameters with the Prandtl number Pr and the Hartmann number Ha. In fact, for the stability of a horizontal liquid layer without magnetic field, the results of Gill [4], obtained with this approximation, are in agreement within a factor two with those of Hart [7,8] obtained by numerical linear stability calculations. As will be shown later, this approximation is still better for our results under magnetic field. When considering that $v_z(z)$ and $\tau_z(z)$ are constants, Eq. (20) has sinusoidal solutions in z. Assuming that the cavity depth H will be approximately half the wavelength in the z direction, the simplest solution will correspond to $\eta = \cos(\pi z)$ in order to have $\psi = 0$ on the boundaries, and the operator Δ can then be replaced by

$$\Delta = -\ell^2 - \pi^2 = -k^2. \quad (21)$$

Then Eq. (20) becomes an algebraic equation

$$(\sigma + k^2)\left(\sigma + \frac{1}{Pr}k^2\right)\ (-k^2\ (\sigma + k^2 + Ha^2) + Ha^2\,\ell^2)k^2 + \ell^2\ (-k^2\ (\sigma + k^2 + Ha^2) + Ha^2\ \ell^2)Gr^2\ Pr\,\bar{\tau}_z + \ell^2 Gr^2\,k^2\bar{v}_z + Ha^2\,\pi^2\left(\sigma + \frac{1}{Pr}k^2\right)(-k^2\ (\sigma + k^2 + Ha^2) + Ha^2\,\ell^2) = 0. \quad (22)$$

In fact, we can remark that the choice $\eta = \cos(\pi z)$ is valid for free–free boundaries, but only approximate for rigid–rigid boundaries, the case considered in this study, as the spanwise velocity disturbance is nonzero at the lower and upper walls. Nevertheless, as already mentioned by Gill [4] in the case without magnetic field, the approximation is rather good and allows to qualitatively reproduce the characteristic behaviors. This will be confirmed in the following

for the case under magnetic field by some comparisons with numerical results obtained by the method developed by Kaddeche [14]. The relevance of this approximate method could be explained by the fact that the instabilities are instabilities of the core flow and not much connected to the flow along the boundaries. We can also remark that the choice $\eta = \cos(\pi z)$ giving $\psi = 0$ on the boundaries also leads to $\theta = 0$ on the boundaries according to Eq. (13). Our approximation will then be correct only for thermally conducting boundaries, which is the case we study in the following.

Since we are interested in oscillatory solutions, σ is taken as a complex number:

$$\sigma = \sigma_r + \mathrm{i}\sigma_i. \tag{23}$$

The condition for the marginal instability is $\sigma_r = 0$. Replacing σ by $\mathrm{i}\sigma_i$ in Eq. (22) and taking the real and imaginary parts equal to zero, will lead to two expressions for σ_i^2. Combining these two expressions, one can obtain the critical value of $Gr(k)$ beyond which the instability occurs, this value being obtained as an explicit function of k, Pr and Ha, namely

$$Gr^2(k) = -\frac{2\,[k^4 + Ha^2\,\pi^2]\,[k^4(1+Pr) + Pr\,Ha^2\,\pi^2]^2}{Pr^2\,k^2\,(k^2-\pi^2)[k^2\bar{v}_z + k^4\bar{\tau}_z(1+Pr) + \bar{\tau}_z Ha^2\,\pi^2 Pr]}. \tag{24}$$

For a practical situation, the values of the Prandtl and the Hartmann numbers are known, and consequently, the corresponding critical value of the Grashof number Gr_c is defined as the minimum of $Gr(k)$ with respect to k: $Gr_c = \mathrm{Min}_{k\in[0,+\infty[}(Gr(k))$. The minimization also gives k_c from which $l_c = \sqrt{k_c^2 - \pi^2}$ and $\lambda_c = 2\pi/l_c$ are deduced. The pulsation σ_i and the frequency $f_c = \sigma_i/2\pi$ are then obtained from one of the previous expressions of σ_i^2.

For the case without magnetic field, i.e., $Ha = 0$, analytical relationships can be obtained:

$$Gr_{c_0} = \frac{\pi^4}{Pr}\sqrt{\frac{(15+3Pr-\chi(Pr))^4}{(Pr^2+6Pr+5)\chi(Pr) - (3Pr^3+Pr^2+41Pr+43)}}, \tag{25}$$

$$\lambda_{c_0} = 4\sqrt{\frac{1+Pr}{11-Pr-\chi(Pr)}}, \tag{26}$$

$$f_{c_0} = \frac{\pi}{8(1+Pr)}\sqrt{\frac{(15+3Pr-\chi(Pr))^2\left(32+31Pr+3Pr^2-Pr\chi(Pr)\right)}{Pr(1-3Pr+\chi(Pr))}}, \tag{27}$$

where $\chi(Pr) = \sqrt{9Pr^2 - 38Pr + 97}$. These expressions can be developed in series for the small Pr limit ($Pr \ll 1$). The relevant scales for the dependence of Gr_{c_0}, λ_{c_0} and f_{c_0} on the Prandtl number are then obtained:

$$Gr_{c_0} \propto \frac{1034}{Pr} + 1280 + O(Pr), \tag{28}$$

$$\lambda_{c_0} \propto 3.728 + 0.359Pr + O(Pr^2), \tag{29}$$

$$f_{c_0} \propto \frac{3.474}{\sqrt{Pr}} + 1.787\sqrt{Pr} + O(\sqrt{Pr}^3). \tag{30}$$

Note that these behaviors, $Gr_{c_0} \propto Pr^{-1}$, $\lambda_{c_0} \propto Pr^0$ and $f_{c_0} \propto Pr^{-1/2}$, are in good agreement with the numerical results of Hart [7,8] and Laure and Roux [10].

When a vertical magnetic field is considered, it is no longer possible to obtain an analytical expression for the critical characteristics. Thus, Gr_c is obtained by minimizing Eq. (24) with respect to k for given values of Prandtl and Hartmann numbers. In Fig. 2, where are plotted the neutral stability curves giving the variation of Gr_c as a function of Ha^2 for various Pr, we can see that Gr_c is close to a linear evolution with Ha^2. This gives a characteristic law $Gr_c - Gr_{c_0} \propto Ha^2$ which is in good agreement with that of Ben Hadid et al. [11] obtained by numerical stability analysis for a cavity with free surface. Note from Fig. 2 that the domain in Ha where this law is well verified seems to diminish as Pr is increased. In Fig. 2 some stability thresholds obtained by numerical stability analysis [14] for $Pr = 0.02$ are also given. We can see that the differences with the corresponding approximate analytical results are reasonable, and that these differences decrease as Ha is increased. This could be related to the fact that the boundary

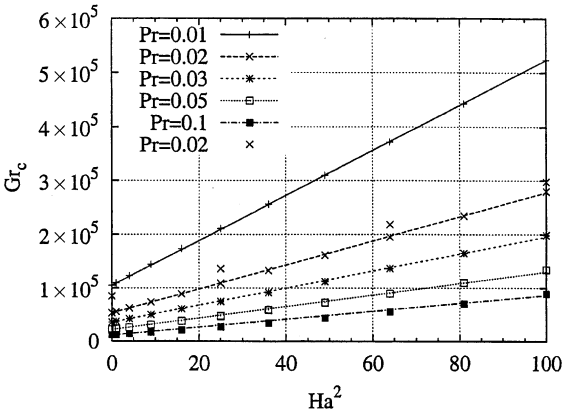

Fig. 2. Variation of Gr_c versus Ha^2 for the oscillatory longitudinal instabilities (different values of the Prandtl number). The lines drawn are straight lines which approximately fit the calculated results. For $Pr = 0.02$ are given four thresholds (indicated by X) obtained by numerical stability calculations with the method developed by Kaddeche [14].

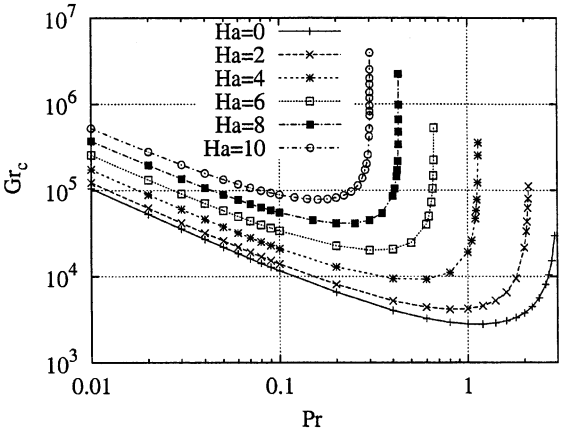

Fig. 3. Variation of Gr_c versus Pr for the oscillatory longitudinal instabilities (different values of the Hartmann number).

layers, which are not well resolved in the model decrease in size as Ha is increased.

The neutral stability curves in the (Gr_c, Pr) plane, given in Fig. 3 for various Ha, show clearly two distinct behaviors depending on the value of the Prandtl number. Indeed, for a given Hartmann number, starting from small Prandtl number values ($Pr \sim 0.01$), when Pr is increased, the critical Grashof number first decreases to reach a minimum at $Pr = Pr_m$, and then increases sharply.

In the range $Pr < Pr_m$, the evolution with Pr is as Pr^{-1} (see Eq. (24) for small Pr), so that the evolution of the critical Grashof number can be summarized by an universal law: $Gr_c - Gr_{c_0} \propto Ha^2\, Pr^{-1}$. In fact, for this range of Pr (assuming $Pr \ll 1$), Eq. (24) can be transformed in a more suitable form, namely

$$Gr(k) = Gr_0(k)\left(1 + Ha^2\left(\frac{k^4 + 4\pi^4}{8\pi^2 k^4}\right)\right) f(k, Ha) \tag{31}$$

with

$$Gr_0(k) = \frac{\pi^2 k^4}{Pr}\frac{\sqrt{32}}{\sqrt{(k^2 - \pi^2)(4\pi^2 - k^2)}}$$

(expression for $Ha = 0$) (32)

and $f(k, Ha)$ such that $f(k, Ha = 0) = 1$ and $0.89 < f(k, Ha) \leqslant 1$ for any Ha and for k in the range deduced from Fig. 6 ($3.5 < k < 4.2$).

For $Pr > Pr_m$, there is a strong increase of the critical Grashof number which occurs earlier and earlier when Ha is increased, indicating that Pr_m is a decreasing function of Ha. This strong increase of Gr_c beyond Pr_m also indicates that there is a limit value Pr_l of Pr beyond which the longitudinal instability disappears. This limit value can be obtained from Eq. (24). The numerator of $Gr^2(k)$ in Eq. (24) being negative, the existence of Gr is conditioned by a negative denominator, i.e.,

$$[k^2 \bar{v}_z + k^4 \bar{\tau}_z(1 + Pr) + \bar{\tau}_z Ha^2 \pi^2 Pr] < 0. \tag{33}$$

Using the fact that $\bar{\tau}_z/\bar{v}_z = -1/4\pi^2$ (thermally conducting boundaries) and $k \geqslant \pi$, Eq. (33) allows to find out $Pr_l(Ha)$, limit between potentially unstable and stable domains, which is given by

$$Pr_l = \frac{3\pi^2}{\pi^2 + Ha^2}. \tag{34}$$

From Eq. (34) it is clear that without magnetic field, oscillatory instabilities can develop only for $Pr < 3$ which is a limit value already obtained by Gill [4]. In Fig. 4, where is displayed the limit given by Eq. (34), we can note that the potentially unstable domain becomes narrower in terms of Prandtl number when Ha is increased. Fig. 4 also shows that for a given Prandtl number there is a limit in terms of Ha for the oscillatory instabilities,

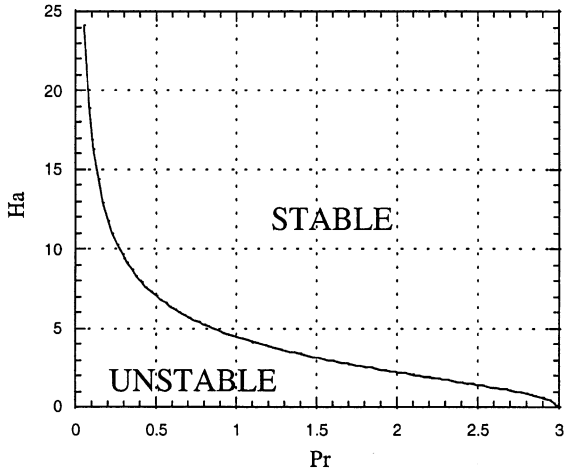

Fig. 4. Representation of the stable and potentially unstable domains (with respect to the oscillatory longitudinal instabilities) in a (Pr, Ha) plane.

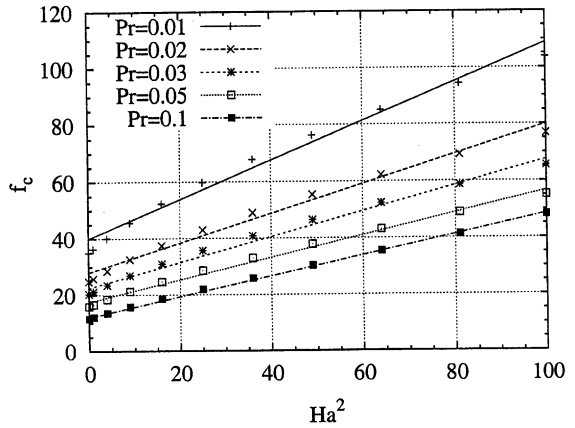

Fig. 5. Variation of the critical oscillation frequency f_c versus Ha^2 for the oscillatory longitudinal instabilities (different values of the Prandtl number). The lines drawn are straight lines which approximately fit the results.

limit noted Ha_l which increases as Pr decreases, namely

$$Ha_l = \pi\sqrt{\frac{3 - Pr}{Pr}}. \tag{35}$$

The effect of a vertical magnetic field on the longitudinal instabilities is also visible in the behavior of the frequency f_c (Fig. 5) which can be approximated by a characteristic law $f_c - f_{c_0} \propto Ha^2\, Pr^{-1/2}$ in the small Pr domain ($Pr \leqslant 0.1$) and of the wavelength λ_c (Fig. 6) which is found as

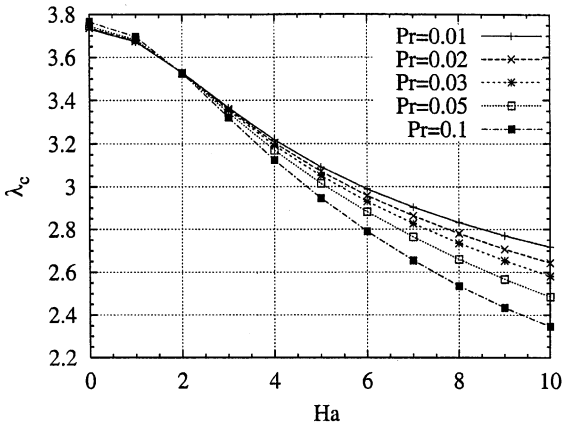

Fig. 6. Variation of the critical wavelength λ_c versus Ha for the oscillatory longitudinal instabilities (different values of the Prandtl number).

a decreasing function of the Hartmann number. This last point indicates that the size of the marginal cells shrinks when increasing the magnetic field strength. Concerning the influence of Pr, λ_c evolves from a very slow increase with Pr for $Ha = 0$ to a more significant decrease for larger Ha.

4. Linear stability analysis for the stationary transverse instabilities

The second type of instabilities which can appear in the shear flow described by Eqs. (7)–(9) correspond to stationary transverse modes which consist of rolls with the axis perpendicular to the basic flow plane (xOz). Due to the fact that these instabilities, also called two-dimensional instabilities, occur in the low Prandtl number range [7,8,10] and that the critical parameters such as the Grashof number and the wavelength remain almost constant for $Pr \to 0$, even in the presence of a magnetic field [11], we will restrict our investigations to the small Prandtl number limit. The analytical approach used in the previous section was not found to be efficient to treat the problem of the transverse instabilities. Introducing the stream function φ in the (xOz) plane, one can write the velocity perturbation components as

$$u = -\varphi_z \quad \text{and} \quad w = \varphi_x. \tag{36}$$

In the small Prandtl number limit, from the linearized Navier–Stokes equations, a single equation for the stream function φ can be derived, namely

$$\frac{\partial}{\partial t}\Delta\varphi + U_0(z)(\varphi_{xzz} + \varphi_{xxx}) - \frac{d^2U_0(z)}{dz^2}\varphi_x = \Delta^2\varphi - Ha^2\varphi_{zz}. \quad (37)$$

We look for solutions of (37) in the following form:

$$\varphi = e^{\sigma t}e^{ihx}\zeta(z). \quad (38)$$

Substituting Eq. (38) into Eq. (37) and noting $U_0(z) = Gr\,v(z)$ and $\sigma = -ihc\,Gr$, one can obtain an ordinary differential equation of order four in z, namely

$$\frac{d^4\zeta}{dz^4} - (2h^2 + Ha^2 + ih\,Gr(v(z) - c))\frac{d^2\zeta}{dz^2} + \left(h^4 + ih\,Gr\left(h^2(v(z) - c) + \frac{d^2v(z)}{dz^2}\right)\right)\zeta = 0. \quad (39)$$

This last differential equation which, except for the magnetic term, is identical to the Orr–Sommerfeld equation, has no exact analytical solution. To solve Eq. (39) we use an approach based on a Taylor development at order 6 which allows to obtain a relevant approximation. The solution which involves four unknown constants has to satisfy the imposed boundary conditions which can be written as

$$\zeta\left(-\frac{1}{2}\right) = \zeta\left(\frac{1}{2}\right) = 0 \quad \text{and}$$
$$\frac{d\zeta}{dz}\left(-\frac{1}{2}\right) = \frac{d\zeta}{dz}\left(\frac{1}{2}\right) = 0. \quad (40)$$

We then obtain a system of four linear equations with four unknowns. In order to find out nonzero solutions, we have to impose that the complex fourth order determinant of this linear system is equal to zero. This procedure leads to a couple of algebraic equations. The first equation obtained from the imaginary part of the determinant gives $c = 0$ which means that the transverse instabilities are stationary, confirming what was already obtained without magnetic field. The second equation obtained from the real part of the determinant allows to obtain the Grashof number $Gr(h, Ha)$ beyond which the transverse instabilities occur, as an explicit function of h and Ha, namely

$$Gr(h, Ha) = \sqrt{\frac{-2\sinh^2(Ha/2)Ha^4N(h, Ha)}{h^2D(h, Ha)}} \quad (41)$$

with

$$N(h, Ha) = h^{12} + A_{10}h^{10} + A_8h^8 + A_6h^6 + A_4h^4 + A_2h^2 + A_0,$$
$$D(h, Ha) = C_6h^6 + C_4h^4 + C_2h^2 + C_0. \quad (42)$$

The coefficients $(A_{2n})_{n=0..5}$ and $(C_{2n})_{n=0..3}$ are given in Appendix B. In order to find out the critical Grashof number beyond which instabilities occur, we have to determine the minimum of the $Gr(h, Ha)$ function with respect to h for different values of Ha. The results are given in Fig. 7 where we can notice that the vertical magnetic field has a strong stabilizing effect on the development of transverse instabilities. Indeed, Gr_c is found to vary exponentially with the square of the Hartmann number, namely, $Gr_c \propto \exp(Ha^2/21.6)$. Note that a similar trend was obtained by Ben Hadid et al. [11] by means of numerical computations in the case of open cavities. Consequently, we can deduce that the vertical magnetic field has a more

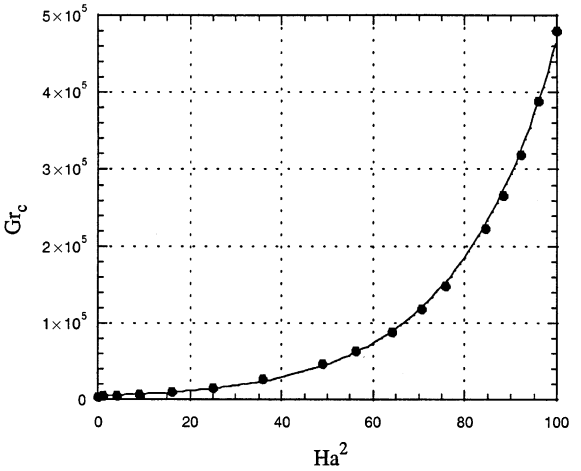

Fig. 7. Variation of Gr_c versus Ha^2 for the transverse instabilities ($Pr = 0$).

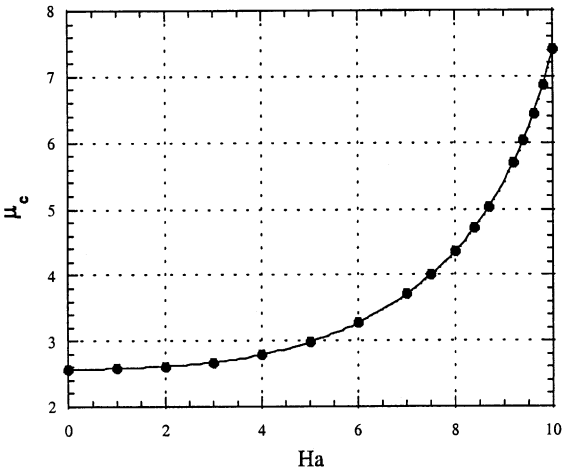

Fig. 8. Variation of the critical wavelength μ_c versus Ha for the transverse instabilities ($Pr = 0$).

significant stabilization effect on the stationary transverse modes than on the oscillatory longitudinal modes. The vertical field can then be seen as favoring the instabilities corresponding to oscillatory longitudinal modes. From Fig. 8, we can also remark that the wavelength $\mu_c = 2\pi/h_c$ increases with Ha indicating the occurrence of longer cells in the cavity.

It is possible to show from Eq. (41) that there is a limit in terms of Ha for the transverse instabilities to appear. $N(h, Ha)$ being positive, the numerator in Eq. (41) is strictly negative. A condition for the instabilities to occur is then that $D(h, Ha)$ is negative. For large h, $D(h, Ha)$ is dominated by $C_6 h^6$ and as $C_6 \geqslant 0$, $D(h, Ha) \geqslant 0$ and so instabilities cannot occur. For smaller h, $D(h, Ha)$ can be negative for small Ha before becoming positive for larger Ha, indicating a domain where instabilities can occur. This domain increases as h decreases, being limited for example by $Ha_l = 6.895$ for $h = 2.5$ (value of the wavenumber for $Ha = 0$), and by $Ha_l = 11.471$ for $h = 0$ (in this case, the limit is given by $C_0 = 0$). Then, in any case, $Ha_l = 11.471$ is the limit beyond which no transverse instability can occur at $Pr = 0$. This limit has been experienced during our calculations of Gr_c, as it has been possible to calculate thresholds up to $Ha = 11.4$, but not for 11.5 and above this value.

5. Concluding remarks

In this study we investigated the effects of a vertical constant magnetic field on the development of oscillatory longitudinal or stationary transverse instabilities in a bounded planar liquid metal layer heated through a horizontal temperature gradient. The most important result that can be pointed out is the strong stabilizing effect of the vertical magnetic field on the development of both longitudinal and transverse instabilities.

For the oscillatory longitudinal modes, the stabilizing effect of the vertical magnetic field on the critical Grashof number scales as $Gr_c - Gr_{c_0} \propto Ha^2$. A similar scale law was found for the oscillation frequencies, $f_c - f_{c_0} \propto Ha^2$. Moreover, for low Prandtl numbers, Gr_c and f_c scale differently with respect to Pr, namely, $Gr_c \propto Pr^{-1}$ and $f_c \propto Pr^{-1/2}$. Consequently, we can deduce the two following scaling laws with respect to Ha and Pr, namely, $Gr_c - Gr_{c_0} \propto Ha^2\, Pr^{-1}$ and $f_c - f_{c_0} \propto Ha^2\, Pr^{-1/2}$. The vertical magnetic field has also an effect on the marginal cells size: we have observed a decrease in the values of the wavelengths which indicates that the marginal cells become narrower when the magnetic field strength is increased. Another aspect of applying a vertical magnetic field is to reduce the potentially unstable domain in terms of Prandtl number. Indeed, when no magnetic field is applied ($Ha = 0$), the instabilities can occur for $Pr < 3$, whereas for $Ha > 0$, instabilities are able to appear only for $Pr < Pr_l(Ha)$, where $Pr_l(Ha)$ is a function decreasing with Ha. This limit can also be viewed as a limit Hartmann number (Ha_l) at given Pr, indicating that the longitudinal instabilities disappear beyond Ha_l.

The vertical magnetic field is seen to have a more significant stabilizing effect on stationary transverse instabilities. Indeed, the corresponding critical Grashof number is seen to scale exponentially with the square of the Hartmann number, namely, $Gr_c \propto \exp(Ha^2/21.6)$. This result indicates that the oscillatory longitudinal modes will become the preferred modes in experiments under magnetic field such as crystal growth processes, when increasing Ha. These transverse instabilities also disappear beyond a limit value of Ha

($Ha_l = 11.471$ for $Pr = 0$). Another important result concerns the effect of the vertical magnetic field on the marginal cells size. Indeed, the marginal cells become wider in the case of the transverse instabilities when increasing Ha, whereas they became narrower in the case of the longitudinal instabilities.

Appendix A

Value of $\bar{v}_z$:

$$\bar{v}_z = \frac{\int_{-1/2}^{1/2}(1/Gr)\,(\mathrm{d}U_0/\mathrm{d}z)\cos^2(\pi z)\mathrm{d}z}{\int_{-1/2}^{1/2}\cos^2(\pi z)\,\mathrm{d}z} = \frac{-1}{4\pi^2 + Ha^2}. \quad (A.1)$$

Value of $\bar{\tau}_z$ given for different boundary conditions:

- For thermally conducting boundaries:

$$\bar{\tau}_z = \frac{\int_{-1/2}^{1/2}\,(1/Gr\,Pr)\,(\mathrm{d}T_0/\mathrm{d}z)\cos^2(\pi z)\,\mathrm{d}z}{\int_{-1/2}^{1/2}\cos^2(\pi z)\,\mathrm{d}z} = \frac{1}{4\pi^2(4\pi^2 + Ha^2)}. \quad (A.2)$$

- For thermally insulating boundaries:

$$\bar{\tau}_z = \frac{1}{Ha^2}\left[\frac{4\pi^2}{Ha^2(4\pi^2 + Ha^2)} + \frac{1}{12} + \frac{1}{4\pi^2} - \frac{\coth(Ha/2)}{2Ha}\right]. \quad (A.3)$$

Appendix B

Values of the different coefficients $(A_{2n})_{n=0..5}$ and $(C_{2n})_{n=0..3}$:

$$A_{10} = 288,$$

$$A_8 = 144\ Ha^2 + 29568,$$

$$A_6 = 23040\ Ha^2 + 1,437,696,$$

$$A_4 = 5760\ Ha^4 + 1,161,216\ Ha^2 + 37,601,280,$$

$$A_2 = 331776\ Ha^4 + 26,542,080\ Ha^2 + 566,231,040,$$

$$A_0 = 55296\ Ha^6 + 6,635,520\ Ha^4 + 283,115,520\ Ha^2 + 4,246,732,800$$

and

$$C_6 = (2\ S - Ha)^2,$$

$$C_4 = S^2\ \left(4\ Ha^2 + 576\right) - S\ Ha\ \left(576 + 10\ Ha^2\right) + 4\ Ha^4 + 144\ Ha^2,$$

$$C_2 = S^2\ (192\ Ha^2 + 23,040) - S\ Ha\ (23,040 + 768\ Ha^2 + 4\ Ha^4) + 4\ Ha^6 + 336\ Ha^4 + 5760\ Ha^2,$$

$$C_0 = S^2\ 221,184 - S\ Ha\ (221,184 + 11,520\ Ha^2 + 96\ Ha^4) + Ha^8 + 144\ Ha^6 + 5760\ Ha^4 + 55,296\ Ha^2.$$

with $S = \sinh(Ha/2)$.

References

[1] D.T.J. Hurle, E. Jakeman, C.P. Johnson, J. Fluid Mech. 64 (1974) 565.
[2] A. Juel, T. Mullin, H. Ben Hadid, D. Henry, J. Fluid Mech. 378 (1999) 97.
[3] L. Davoust, M.D. Cowley, R. Moreau, R. Bolcato, J. Fluid Mech. 400 (1999) 59.
[4] A.E. Gill, J. Fluid Mech. 64 (1974) 577.
[5] G.Z. Gershuni, E.M. Zhukhovitskii, Zh. Eksp. Teor. Fiz (Transl. Sov. Phys. JETP) 34 (3) (1958) 675.
[6] R.V. Birikh, et al., Magn. Gidrodin. 1 (1978) 30.
[7] J.E. Hart, J. Atmos. Sci. 29 (1972) 687.
[8] J.E. Hart, J. Fluid Mech. 132 (1983) 271.
[9] M.K. Smith, S.H. Davis, J. Fluid Mech. 132 (1983) 119.
[10] P. Laure, B. Roux, J. Crystal Growth 97 (1989) 226.
[11] H. Ben Hadid, D. Henry, S. Kaddeche, J. Fluid Mech. 333 (1997) 23.
[12] J. Priede, G. Gerbeth, J. Fluid Mech. 404 (2000) 211.
[13] S. Kaddeche, H. Ben Hadid, T. Putelat, D. Henry, J. Crystal Growth (Part 2) 242 (2002) 501.
[14] S. Kaddeche, Ph.D. Thesis, Ecole Centrale de Lyon, 1995.